We are IntechOpen,
the world's leading publisher of Open Access books
Built by scientists, for scientists

4,800
Open access books available

122,000
International authors and editors

135M
Downloads

Our authors are among the

154
Countries delivered to

TOP 1%
most cited scientists

12.2%
Contributors from top 500 universities

CLARIVATE ANALYTICS

BOOK CITATION INDEX

INDEXED

WEB OF SCIENCE™

Selection of our books indexed in the Book Citation Index
in Web of Science™ Core Collection (BKCI)

Interested in publishing with us?
Contact book.department@intechopen.com

Numbers displayed above are based on latest data collected.
For more information visit www.intechopen.com

Stopped-Flow Studies of the Formation of Organic Nanocrystals in the Reprecipitation Method

Daniel Oliveira[1], Koichi Baba[2], Winfried Teizer[1,3], Hitoshi Kasai[1,4],
Hidetoshi Oikawa[1] and Hachiro Nakanishi[1]
[1]Tohoku University,
[2]Osaka University,
[3]Texas A&M University,
[4]PRESTO, Japan Science and Technology
[1,2,4]Japan
[3]United States

1. Introduction

Interest in organic nanoparticles is rapidly growing in the scientific community as it is now clear their potential impact in several attractive economic fields, in special their applications as pharmaceutically active organic compounds (Chen & Zhang, 2006), printing inks (Magdassi & Moshe, 2003) and color filters (Miyashita et al., 2008). Accordingly, a recent report published in BBC Research estimated that by 2015 the global demand for nano-related goods could be higher than US$ 2.4 trillion (McWilliams, 2010). Moreover, the author predicted that the economic power of the nanotechnology industry could be greater than those attained almost a decade ago by both the telecommunication and information technology industries. It is thus hardly surprising that chemical industries need new and reliable methods directed to the production of organic nanoparticles. Furthermore, sizes of prepared organic nanocrystals must be carefully controlled as the properties of materials are strongly dependent on the size of the particles of the materials (Auweter et al., 1999; Burda et al., 2005; Horn & Rieger, 2001).

Methods used for the preparation of organic nanoparticles are primarily based on either precipitation, milling, or through chemical reaction techniques. Unfortunately, the former two techniques proved to be less attractive in manufacturing organic nanosized materials, as milling techniques rely on applying an extremely high mechanical energy on the system leading to structural changes of the crystal (Bilgili et al., 2006; Peters, 1996); and synthetic approaches are based on considerable exhaustive, and therefore time consuming synthetic routes (Spatz et al., 1999; Sugimoto et al., 2002). As a consequence, methods which rely on solubility changes to induce nanoparticle formation are lately becoming more attractive. Among these methods (Frendler, 1987; Hayashi et al., 2007; Ibanez et al., 1998; Kasai et al., 1992; Kasai et al., 1996), a simple and convenient technique proved to be particularly effective for the preparation of organic nanoparticle dispersion, the so-called "reprecipitation method" (Kasai et al., 1992; Kasai et al., 1996).

In the reprecipitation method, a dilute solution of a target compound prepared on a water-soluble organic solvent is injected into vigorously stirred water as a poor solubility medium. As the organic solvent disperses, the sudden change in the solubility of the target compound causes it to precipitate in the form of dispersed nanoparticles in an aqueous medium. The reprecipitation method has the advantage of producing nanodispersed systems under mild conditions, a great benefit when considering that the vast majority of organic compounds are thermally unstable.

The physical properties of nanoparticles differ significantly from those of their related bulk crystals due to the changes in lattice state caused by an increase in the surface area of nanoparticles, and consequently, to lattice softening (Masuhara et al., 2002). It is believed that the lattice softening results in weaker interaction between adjacent molecules, ultimately resulting in wider band gaps (Masuhara et al., 2002). For that reason it is no surprise that a technique employed for organic nanoparticles formation must be able to precisely control the size of prepared crystals.

Even though there is vast literature available on the size-controlled formation, characterization, and application of a wide variety of nanoparticles, little attention has been paid to the kinetics of organic nanosized crystal growth; in particular, little is known about nucleation, as it is experimentally difficult to investigate such a phenomenon given the time frame of the process. Tiemann and coworkers systematically studied the early stages of nanoparticle growth (Tiemann et al., 2005; Tiemann et al., 2006; Tiemann et al., 2008) unfortunately, their investigations were restricted to inorganic nanoparticles, which as previously stated, indicates the limited understanding of organic nanoparticles when compared with their inorganic counterpart.

Following the initial work by Van Keuren et al. on the kinetics of the formation of organic nanocrystals (Van Keuren et al., 2001), Mori and coworkers were able to directly observe the formation of organic nanoparticles by the reprecipitation method using stopped-flow UV-Visible absorption spectroscopy (Mori et al., 2009). Authors quantitatively demonstrated that the kinetics of the reprecipitation process is governed by the classical nucleation theory (Chaikin & Lubensky, 1995; Debenedetti et al., 1996; Kashchiev & van Rosmalens, 2003; Laaksonen et al., 1995). Essentially, the classical nucleation theory states that nucleation succeeds through a supersaturated solution, where nuclei are formed by monomers clustering one molecule at a time to a single cluster.

This seminal work conducted by Mori and colleagues is of utmost importance as it correlated for the first time the mechanism of the reprecipitation process and a known nucleation model. However, it is not yet clear whether such a model can be used to explain the reprecipitation mechanism for a wider class of systems undergoing nanocrystallization. To better comprehend the mechanism of organic nanoparticle formation (and hence, control such formation), the classical nucleation theory must be tested to determine whether it can explain changes in nanocrystallization kinetics while varying several parameters of the reprecipitation method. In this chapter, the stopped-flow UV-Visible absorption spectroscopy technique will be used to systematically investigate the growth of several organic nanoparticles in the millisecond time regime and assert if the kinetics of the nanoparticle formation process obeys the classical nucleation theory.

Of utmost importance is not only to control organic nanocrystal formation, but also to precisely manipulate sizes of produced nanocrystals. Unfortunately no literature report shows the use of organic molecules as additives to induce size-controllable nanocrystallization of a desired organic compound. It will also be addressed in this chapter

a novel technique to fabricate organic nanocrystals (here, perylene nanocrystals) with different sizes by employing N,N′-bis(2,6-dimethylphenyl)-3,4,9,10–perylenedicarboxyimide, or simply DMPBI, as an additive in the reprecipitation method. The choice of DMPBI as the additive to study the changes induced in the reprecipitation process of perylene was due to the structural similarity between both organic compounds, i.e., perylene and DMPBI. By monitoring the formation of perylene nanoparticles with the aid of stopped-flow UV-Visible absorption spectroscopy, results suggest that DMPBI molecules act as seeds in the nucleation process, allowing for seed-mediated perylene nanosized crystal growth, increasing nanocrystallization rates, and thus, altering the size of the prepared nanoparticles.

2. Experimental procedure

The sizes of perylene nanoparticles were obtained using the JEOL JSM-6700F scanning electron microscope (SEM) instrument, and the Malvern ZetaSizer Nano-ZS dynamic light scattering (DLS) technique. UV–visible absorption spectroscopy was performed using a Unisoku RSP-1000 stopped-flow spectrometer designed with a photodiode array detector. In order to simulate the reprecipitation method, the injected solution should be fixed at different ratios (Kasai et al., 1992; Kasai et al., 1996); therefore, a mixing ratio of 1:9 (water soluble solvent: water) was achieved by employing two syringes of different sizes. For each run, 41 μL (target compound in organic solvent) and 342 μL (water) were mixed in a spherical mixer and then used to fill a rectangular observation chamber (1 mm optical path length cell). Changes in absorbance were monitored every millisecond for a total of 500 ms. The dead time of the instrument was calculated to be about 4 ms (Tonomura et al., 1978). All collected data were referenced against those of purified water.

3. Results and discussion

Fig. 1 shows the UV-visible absorption spectra acquired with the stopped-flow instrument, where 0.10 mmol L^{-1} perylene dissolved in acetone was mixed with water and its absorption spectra were measured for 500 ms at 1 ms intervals (for clarity, only spectra obtained during the first 200 ms were plotted). Observation of the figure shows a clear pattern concerning the time-resolved absorption spectra of perylene, that is, the disappearance of the absorption band at 405 and 432 nm is occurring as a new absorption band centered at 448 nm is being formed. Earlier studies focused on the preparation of organic nanoparticles showed there is a red-shift in the perylene absorption band when nanocrystals were formed though the reprecipitation method (Kasai et al., 1992; Kasai et al., 1996). Authors concluded that the observed re-shift was due to the formation of aggregated species (An et al., 2002; Fu & Yao, 2001; Kang et al., 2007; Van Keuren et al., 2008; Wang et al., 2005). One can thus fairly assume that the increase in the intensity of the 448 nm band is due to the generation of perylene nanoparticles, while the decrease in the intensity of both the 405 and 432 nm band corresponds to the disappearance of perylene monomers. Also, it is important to point out the existence of an isosbestic point at 444 nm, indicating that only two species with distinct absorption properties are present in the mixture, that is, perylene monomers and perylene nanocrystals.

Using the data shown in the figure, it is possible to calculate the rate constant of nanoparticle formation by either the rate of increase in the area of the nanoparticle band (at
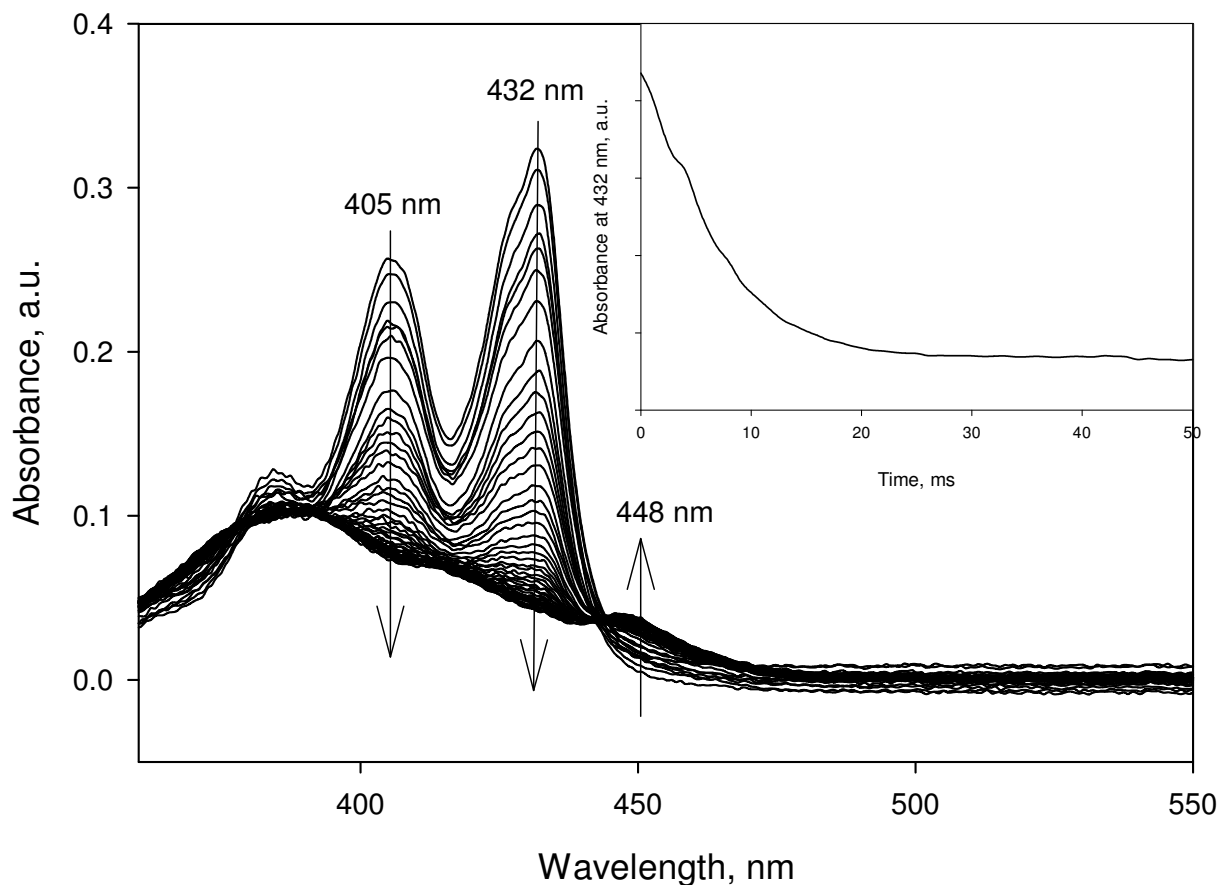
Fig. 1. Time-resolved absorption spectra of perylene in acetone (0.1 mmol L^{-1}) mixed with water. Inset shows the absorbance intensity at 432 nm as a function of time

448 nm) or by the rate of decrease in the area of the monomer band (either at 405, or at 432 nm). The latter band at 432 nm will be used throughout this chapter to calculate nanocrystallization rates because, as seen in the figure, the intensity of such band is much higher than the intensity of the nanoparticle band (and of the 405 nm band), and therefore, more accurate data is expected to be obtained. The Fig. 1 inset shows the intensity absorbance decay at 432 nm as a function of time during the first 50 ms after reprecipitation, corresponding to perylene monomers consumption. Calculation of rate of perylene nanoparticle formation is defined as the inverse of the time for the monomer absorbance to decrease to 1/e from its initial absorbance (Mori et al., 2009). It is important to point out that the formation of perylene nanocrystals by the reprecipitation method is completed within tens of milliseconds.

A key parameter in understanding the nanocrystallization mechanism of organic compounds is the supersaturation ratio, defined as C/C$_e$, where C is the initial target compound concentration and C$_e$ is the solubility of that target compound in the water/organic solvent mixture. Therefore, one can change the type of target compound, the type of solvent, temperature, and concentration in order to gain better insight into the reprecipitation process. With that in mind, perylene solutions were prepared at three different concentrations (0.05, 0.1, and 0.2 mmol L^{-1}) and their time-resolved absorbance spectra measured every 5 degree Celsius from 5 to 50 °C. After spectral acquisition, the rate of nanoparticle formation at each concentration and temperature was calculated on the basis

of the decrease in the intensity of the 432 nm monomer peak (as described above). Fig. 2 shows the rates of nanoparticle formation plotted against temperature for the three distinct perylene concentrations. In the figure, each data point is the average of three individual rate constant determinations.
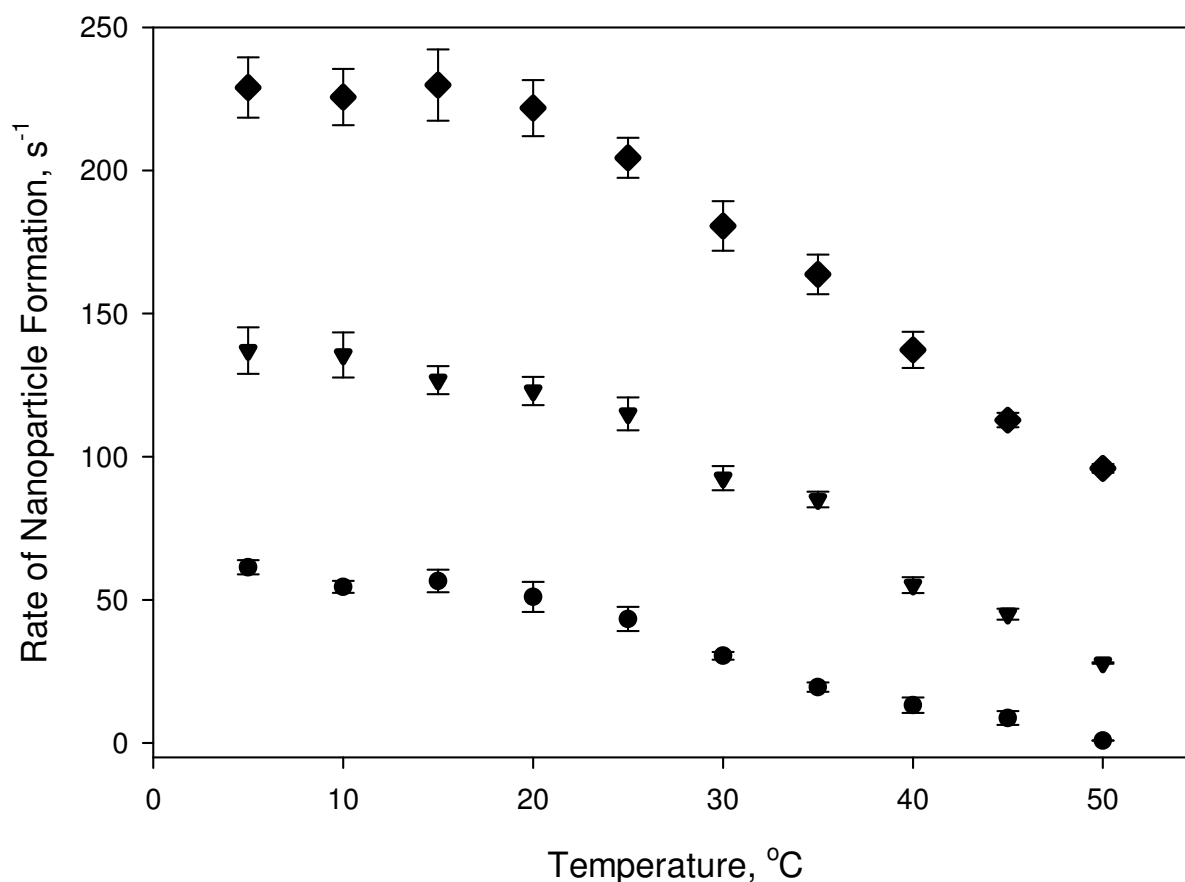

Fig. 2. Rates of nanoparticle formation as a function of temperature for perylene 0.05 mmol L^{-1} (circles), perylene 0.1 mmol L^{-1} (triangles) and perylene 0.2 mmol L^{-1} (diamonds). Solutions were prepared in acetone and mixed with water

Classical nucleation theory predicts that at high supersaturation ratios, molecules will rapidly aggregate and crystal growth will occur at a higher rate through the aggregation of the nucleated particles (Kashchiev & van Rosmalens, 2003). Moreover, the nanoparticle growth process is associated with a decrease in monomer concentration; as a consequence, additional amount of the organic compound must be added or temperature must be reduced to sustain supersaturation. Consequently, as temperature increases, nanoparticle formation rate decreases (at higher temperatures the solubility of the target compound in water increases), which leads to a decrease in supersaturation ratio and ultimately to a decrease in the rate.

Classical nucleation theory also predicts increasing critical nucleus size with increasing temperature, so that the formation of stable nuclei becomes increasingly harder at elevated temperatures. Such a phenomenon, accompanied by the higher cluster diffusivities at elevated temperatures, will result in lower rates of nanoparticle formation, as seen in Fig. 2. The distinctive pattern observed in Fig. 2 (lower nanoparticle formation rates at higher concentrations) is thus in agreement with the classical nucleation theory.

After the dependence of perylene nanoparticle formation as a function of concentration and temperature was successfully obtained and correlated with the classical nucleation theory, studies with other types of low-molecular-weight aromatic compounds shall provide additional information on the nanocrystallization mechanism of organic materials. Hence, the nanoparticle formation processes for anthracene and benzo[a]pyrene were also evaluated using the stopped-flow apparatus. Fig. 3 shows the temporal evolution absorption spectra obtained with the stopped-flow system for anthracene [Fig. 3(A)], and benzo[a]pyrene [Fig. 3(B)]. Both compounds were dissolved in acetone (0.1 mmol L^{-1}) and mixed with purified water in a 1:9 volume ratio. For simplicity, only the spectra acquired during the first 200 ms at 1 ms intervals were plotted.
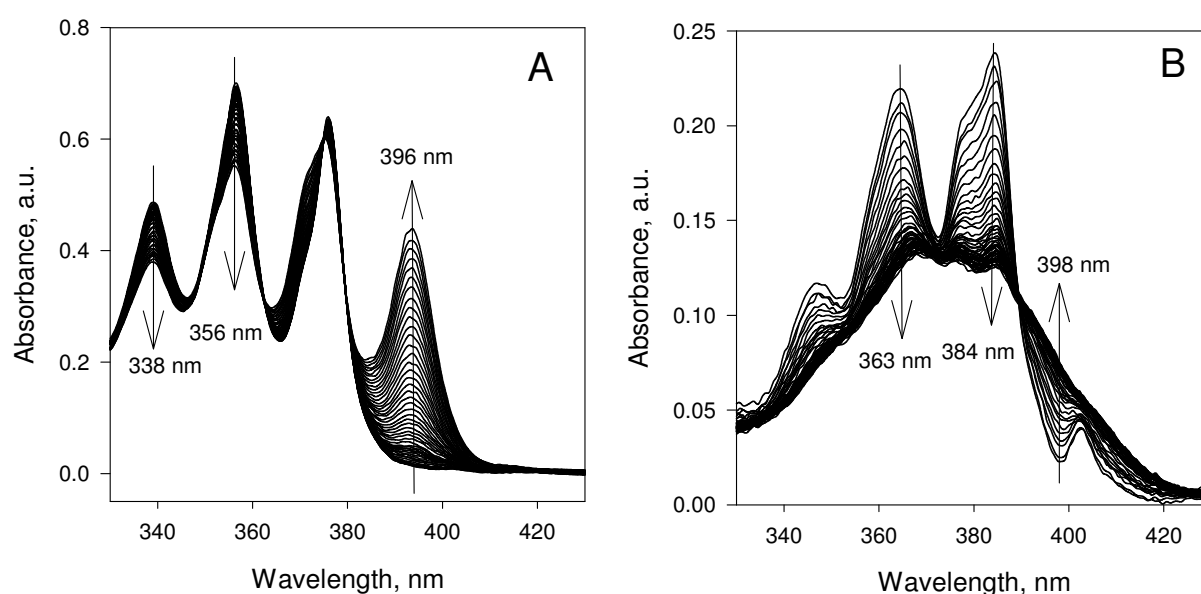

Fig. 3. Time-resolved absorption spectra of (A) anthracene in acetone (0.1 mmol L^{-1}) mixed with water; and (B) benzo[a]pyrene in acetone (0.1 mmol L^{-1}) mixed with water

Similarly as observed with perylene (Fig. 1), anthracene and benzo[a]pyrene shows strong time-dependent absorption spectra. The spectra of anthracene [(Fig. 3(A)] are marked by a decrease in the intensities of the absorption peaks at 338 and 356 nm (anthracene monomers), and by the formation of an absorption peak at 396 nm (anthracene nanoparticles). In addition, the absorption monomer peak at 376 nm gradually vanishes and blue shifts to a new anthracene nanoparticle peak at 371 nm. The time-dependent absorption spectra of benzo[a]pyrene [Fig. 3(B)] follow similar behavior, i.e., monomer bands at 363 and 384 nm decrease in intensity, accompanied by an increase in the intensity of the absorption peak at approximately 398 nm, the benzo[a]pyrene nanoparticle band.

Even though nanoparticle formation of anthracene and benzo[a]pyrene through the reprecipitation method was previously studied (Chung et al., 2006), no studies accounted the kinetics of the process. After confirmation that such nanocrystallization indeed occurs (illustrated on Fig. 3), further kinetic insight can be achieved if, as previously performed, the rate of nanoparticle formation is studied as a function of temperature. Fig. 4 shows such data for anthracene and benzo[a]pyrene, as well as for perylene (replotted from Fig. 2). Nanocrystallization rate was calculated on the basis of the 384 and 356 nm peak decays, for benzo[a]pyrene and anthracene, respectively. Each displayed data point is an average of

three separate rate determinations. As observed in the figure, the rate of nanoparticle formation is clearly dependent on the type of target organic compound and the temperature of the process.
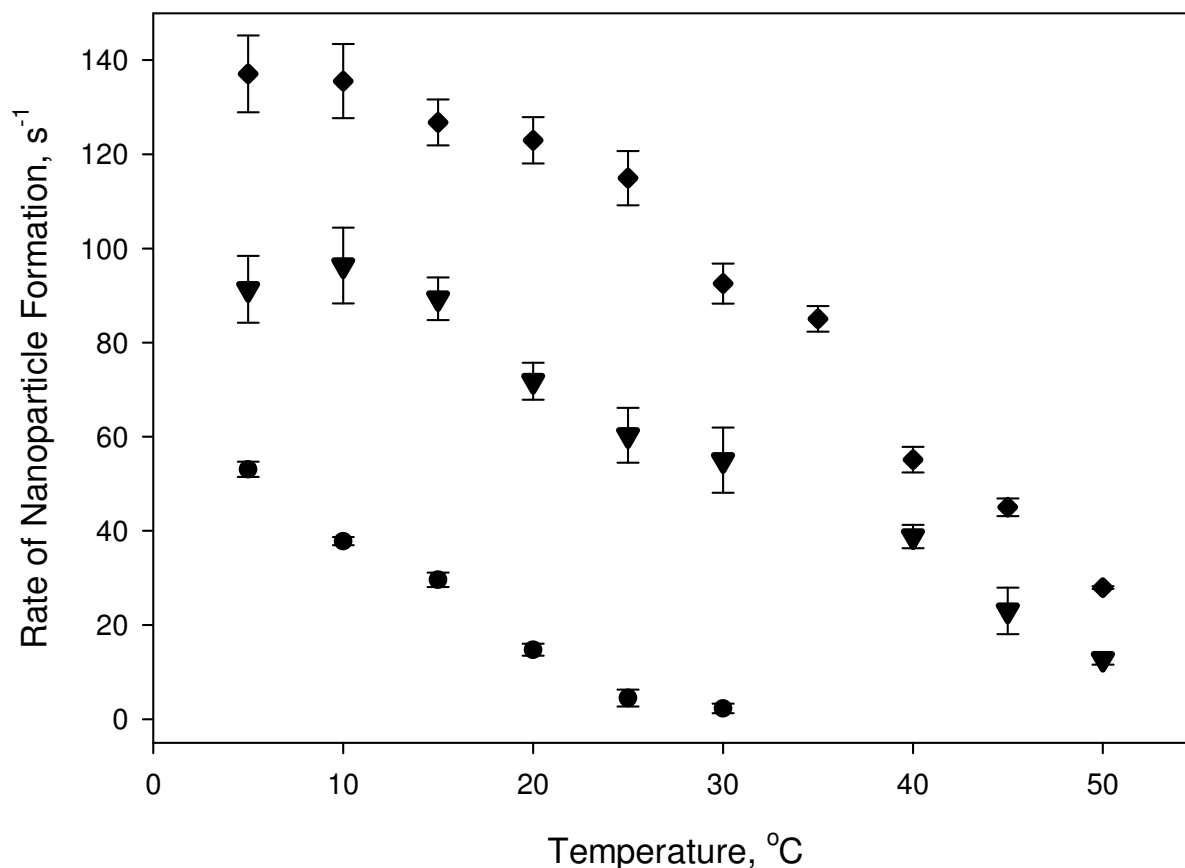

Fig. 4. Rates of nanoparticle formation as a function of temperature for perylene 0.1 mmol L^{-1} (diamonds), benzo[a]pyrene 0.1 mmol L^{-1} (triangles), and anthracene 0.1 mmol L^{-1} (circles). Solutions were prepared in acetone and mixed with water

It was previously stated that supersaturation ratio is a key parameter for understanding rates of nanocrystal formation. As supersaturation ratio is a function of organic compound solubility, the trend observed in Fig. 4 can be explained by correlating the solubility in water of the three organic compounds with their corresponding formation rates. Being perylene the least compound soluble in water [4.2 x 10^{-10} moles/L (Eisenbrand et al., 1970)] it will have the highest supersaturation ratio, and consequently the highest nanoparticle formation rate. In contrast, anthracene, the most soluble in water [2.4 x 10^{-7} moles/L (Eisenbrand et al., 1970)], will have the lowest supersaturation ratio and thus the lowest nanocrystallization rate. Possessing solubility between those of the two compounds, benzo[a]pyrene [(2.0 x 10^{-9} moles/L (Eisenbrand et al., 1970)] is expected to have an intermediate supersaturation ratio and hence an intermediate formation rate, as consistently observed in Fig. 4.

Examining the temperature influence on nanocrystallization rates, the solubility of benzo[a]pyrene increases nearly fivefold when the system is heated from 20 to 35 °C, namely from 2.0 x 10^{-9} moles/L (Eisenbrand et al., 1970) to 1.1 x 10^{-8} moles/L (Blyshak et al., 1989). Interestingly, for organic molecules with a higher water solubility (i.e., anthracene), the effect of temperature is even higher. At 35 °C, the solubility of anthracene is 3.5 x 10^{-7}

moles/L (Blyshak et al., 1989), which is one order of magnitude higher than that of benzo[a]pyrene at an equivalent temperature, and thus nanoparticle formation is observed at a considerable lower rate, as shown in Fig. 4.

Since the effects of concentration and solubility on nanocrystallization rates of organic materials turned out to be in accordance with the classical nucleation theory, the solvent on which organic compounds are dissolved can be varied to test its affect on nanocrystallization rates. Accordingly, perylene was dissolved in two other water miscible solvents, namely, ethanol and tetrahydrofuran (THF) and compared to results previously obtained with acetone as the solvent. Perylene solution of 0.1 mmol L^{-1} was prepared in both solvents, and by using the stopped-flow instrument, perylene nanoparticle formation rate was calculated and plotted in Fig. 5. Perylene 0.1 mmol L^{-1} in acetone was replotted from Fig. 2, where each data point is the average of three individual rate constant determinations.

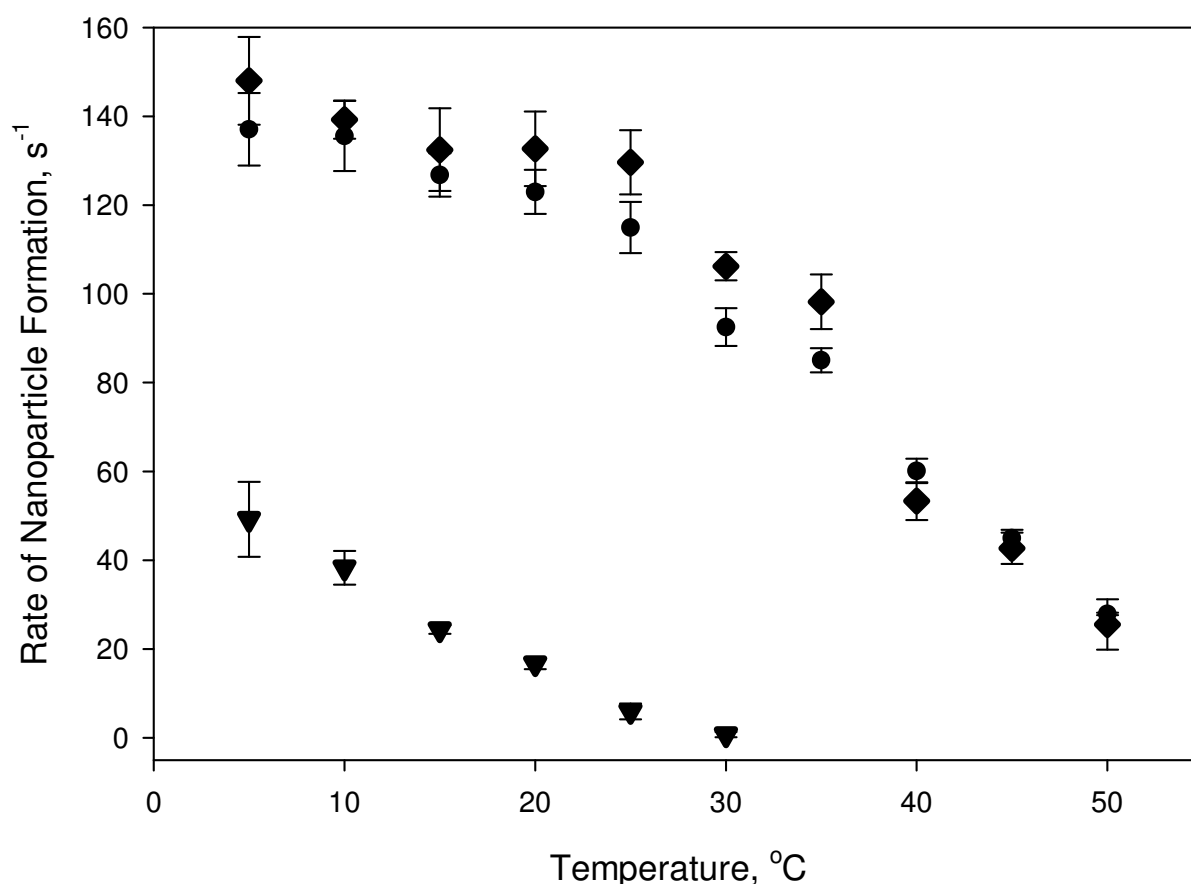Fig. 5. Rates of nanoparticle formation as a function of temperature for perylene
0.1 mmol L^{-1} dissolved in ethanol (diamonds), acetone (circles), and tetrahydrofuran
(triangles) mixed with water

Results visualized in Fig. 5 are strikingly similar with those obtained while varying the type of organic molecule (Fig. 4). Analysis of Fig. 5 shows, as previously observed in Fig. 4, that the dependence of rate of perylene nanoparticle formation on a given parameter (here the type of water-soluble solvent) is considerable strong. Consequently, on the basis of the classical nucleation theory, it is presumed that the same parameter can be used in understanding both results, i.e., solubility.

The solubilities of perylene in ethanol, acetone, and THF were experimentally determined by UV-visible spectroscopic analysis to be 3.7×10^{-4}, 4.1×10^{-3}, and 2.8×10^{-2} moles/L, respectively. As shown in Fig. 5, the rate of perylene nanocrystal formation is in accordance with the solubility of perylene in an organic solvent, that is, the rate increases in the order from the solvent where perylene is most soluble (THF) to the solvent where it is least soluble (ethanol). Bearing in mind that a fixed volume ratio of 1:9 (organic solvent: water) is used when injecting the perylene solution into the aqueous system, it is expected that the solubility of perylene in water will increase as the solubility of perylene in the organic solvent increases, as a consequence of the organic solvent acting as a solubilizing agent (Nyssen et al., 1987). This in turn leads to low supersaturation rates and thus low nanocrystallization rates, as observed in the THF system.

Indeed results presented in Figs. 2, 4 and 5 indicate that indeed organic nanocrystal formation follows the classical nucleation theory. Although it is tempting to conclude that the classical nucleation theory can be used to comprehensively describe organic material nanocrystallization, such proposal is considered to be over simplistic, as it does not take into account several other factors. As an example, a study conducted by Chung and coworkers shows the effect of organic solvent dielectric constant on the reprecipitation method (Chung et al., 2006). Authors demonstrated that cluster concentrations are higher for solvents with larger dielectric constants, because of better organic solvent dispersibilities of such solvents in water. Therefore, the solubility of organic solvent in water may have a prominent effect on the rate of nanocrystallization, as a result of the fast mixing between the two phases. The dielectric constants of ethanol, acetone, and THF are 24.6, 20.7, and 7.6 (Vogel et al., 1996), respectively (at room temperature). Fig. 5 shows the rates to be in accordance with the dielectric constants; ethanol, having the largest dielectric constant, offers a faster transport for perylene molecules to get in contact with the water phase (i.e., highest cluster concentrations) and thus the highest rates. Moreover, the similarity between the nanoparticle formation rates observed when perylene is dissolved in ethanol and acetone is better explained when taking dielectric constant into account. As the solubility of perylene in ethanol is one order of magnitude lower than that in acetone, one would expect the formation rate of perylene to be considerably higher than that shown in Fig. 5, which could be associated with the similar dielectric constants of the two solvents.

Despite the unfortunate lack of studies concerning the mechanism of nanosized organic crystal formation, it could be quantitatively suggested here that the kinetics of the nanoparticle formation process for several types of aromatic organic compounds under several different experimental gross conditions obeys the classical nucleation theory (Oliveira et al., 2009). However, for practical purposes, as important as understanding the mechanism of nanocrystal formation it is the capacity to manipulate its size.

The reprecipitation method has already been subject to several studies focused on the fabrication of size-controllable organic nanoparticles. Among the main parameters which can be controlled in order to manipulate the size of nanoparticles, concentration of the target compound (Katagi et al., 1996), medium temperature (Kasai et al., 1998), and also applied microwave irradiation (Baba et al., 2007) were found to be the most effectives. Now, a novel method to fabricate organic nanocrystals (exemplified by perylene) with different sizes by employing N,N'-bis (2,6-dimethylphenyl) - 3,4,9,10 – perylenedicarboxyimide (DMPBI) as an additive in the reprecipitation method is addressed in the remaining of this chapter.

It was found that adding DMPBI to a solution of perylene led to changes in its nanoparticle formation rate when undergoing reprecipitation in water. Fig. 6 shows the time resolved

absorption spectra of 0.20 mmol L^{-1} perylene in acetone with the addition of 10% (0.02 mmol L^{-1}) DMPBI. It is seen that the basic features of perylene monomer disappearance and nanocrystal appearance are consistent with those illustrated in Fig. 1; also, no shift in either absorption bands is noticed. However, it is observed that monomer molecules are consumed faster, which indicates that the nanocrystallization of perylene is occurring at higher rates with the presence of 10% added DMPBI. Such statement can be readily reached by comparing the insets in Figs. 1 and 6, where a steeper decrease in the intensity of the 432 nm peak shown in Fig. 6 indicates faster rates of perylene monomer consumption in the presence of DMPBI.
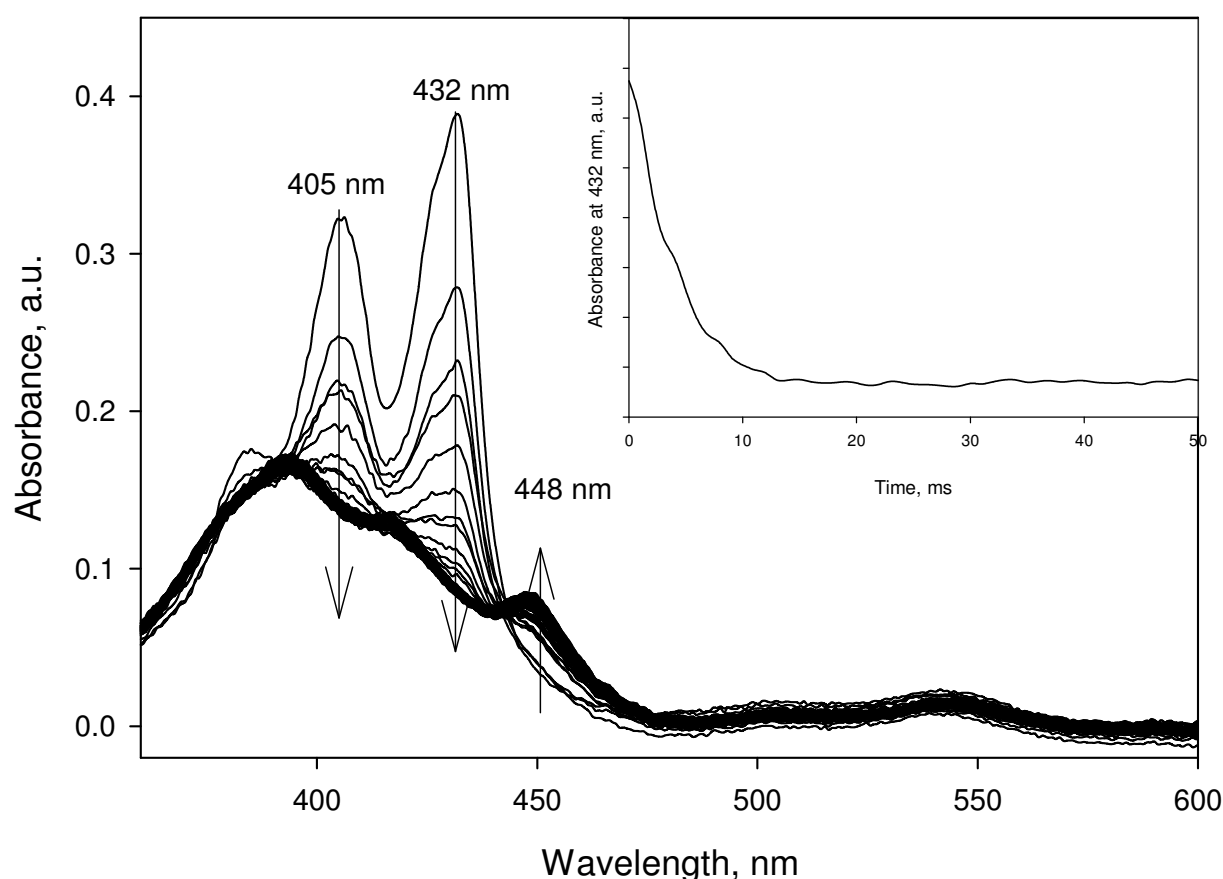
Fig. 6. Time-resolved absorption spectra of perylene 0.2 mmol L^{-1} in acetone with 10 % added DMPBI mixed with water. Inset shows the absorbance intensity at 432 nm as a function of time

Since the decrease in the intensity of the 432 nm band is used for nanoparticle formation rate calculation, the time resolved absorption spectra of DMPBI cannot be overlapping, and hence interfering, with that spectral region. To determine whether that is the case, Fig. 7 was plotted to visualize the temporal evolution absorption spectra obtained with the stopped-flow system for DMPBI (0.10 mmol L^{-1}) after reprecipitation in water. For reasons of simplicity, it is only plotted the spectra acquired during the first 200 ms at 1 ms intervals.

The absorption spectra for DMPBI, as seen in Fig. 7, is also strongly time dependent. Although a strong variation is noticed during the first tens of milliseconds after the mixing with water, a decrease in the area of the monomer band followed by an increase in the area
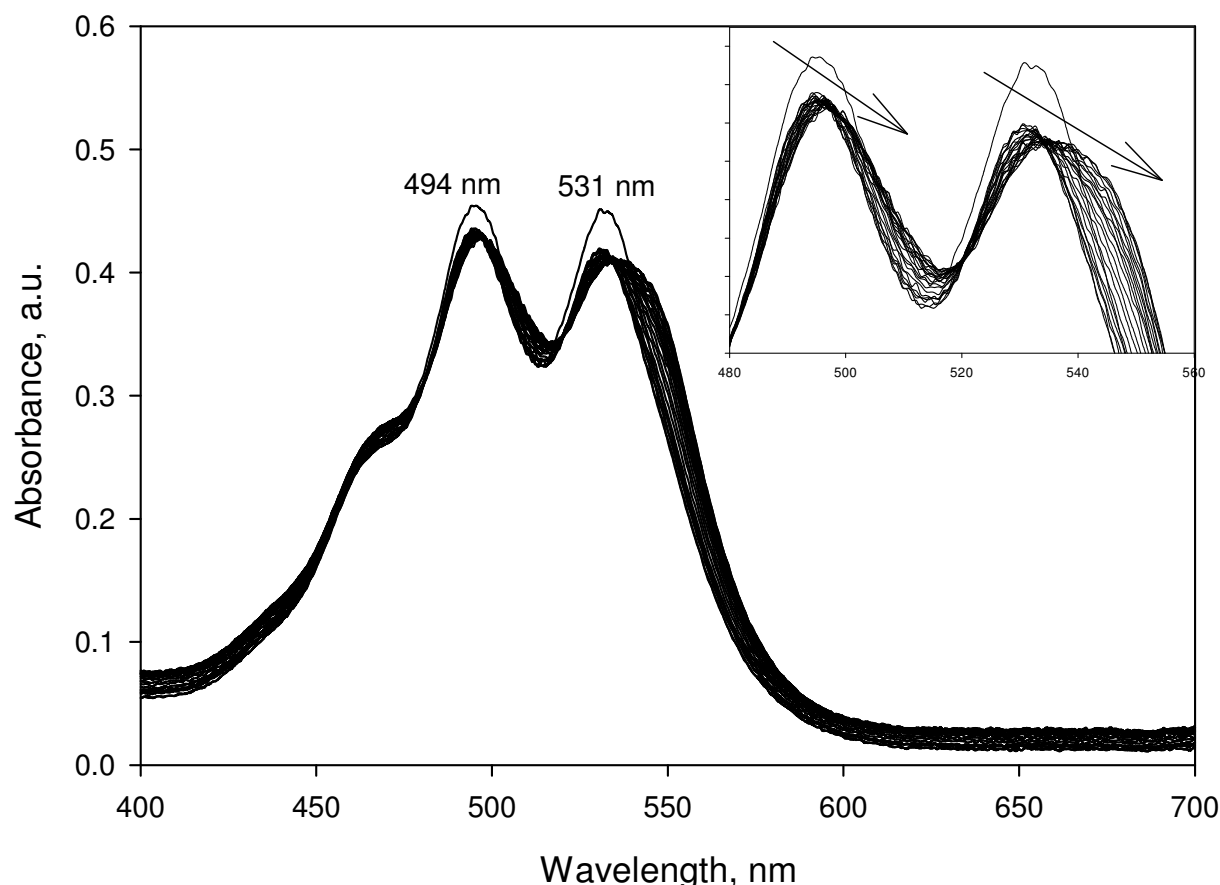
Fig. 7. Time-resolved absorption spectra of 0.1 mmol L^{-1} N,N'-bis (2,6-dimethylphenyl)-3,4,9,10 - perylenedicarboxyimide (DMPBI) mixed with water. Inset shows magnification of the absorbance profile from 480 to 560 nm

of the nanoparticle band is not as perceptible as in the case of perylene (Fig. 1), anthracene or benzo[a]pyrene (Fig. 3). Both absorption bands at 494 and 531 nm display similar behavior, that is, absorption monomer peaks are gradually disappearing and red shifting to a new DMPBI nanoparticle band. Calculation of DMPBI nanoparticle formation rate is an arduous task to accomplish because the decay in the intensity of absorbance is particularly low in magnitude. More importantly, the nanoparticle absorption band is created while overlapping with the monomer band, being those absorption maxima only a few nanometers apart. Consequently, kinetics decay curves necessary for the calculation of nanoparticle formation rates cannot be precisely isolated, and thus, obtained time decay curves are not suitable for accurate and reliable rate determination.

Observation of Fig. 7 clearly indicates that the DMPBI absorbance pattern does not interfere with perylene molecules absorbance (Fig. 1), especially at the 432 nm spectral range which is used for calculation of perylene nanocrystallization rates. As a result, rate constant calculation at 432 nm can be assigned solely to perylene molecules, and thus, the presence of DMPBI molecules in the reaction environment seems to accelerate rates of perylene nanocrystallization. In order to confirm if DMPBI is indeed responsible for the faster rate of perylene nanocrystal formation, a set consisting of seven solution of 0.20 mmol L^{-1} perylene in acetone with various amount of added DMPBI was prepared. Exact compositions of such

solutions are displayed in Table 1. As listed, each solution has the same perylene concentration (0.20 mmol L^{-1}) but different DMPBI concentrations, ranging from 0.00 to 0.06 mmol L^{-1}.

DMPBI %	Concentration (mM)	
	Perylene	DMPBI
0%	0.200	0.000
1%	0.200	0.002
2%	0.200	0.004
5%	0.200	0.010
10%	0.200	0.020
20%	0.200	0.040
30%	0.200	0.060

Table 1. Composition of measured perylene solutions with added DMPBI percentage

Each solution displayed in Table 1 had its corresponding UV-visible absorption spectrum obtained with the stopped flow system after reprecipitation with water. Fig. 8 shows absorption spectra for the 7 solutions measured during the first 500 ms after mixing with water at 1 ms intervals; spectra A-F in the figure corresponds to solutions with 1 to 30% added DMPBI, respectively. The first solution shown on the table, i.e., 0% DMPBI, was not plotted on Fig. 8 as it is displayed in Fig. 1. It is readily observed from the decrease in the intensity of the 432 monomer peak that perylene undergoes nanocrystallization regardless of the DMPBI percentage in solution. Also, the intensity and shape of the 432 nm peak is clearly varying with addition of DMPBI. More importantly, inset in each graph indicates that perylene monomers are faster consumed in solution as the DMPBI concentration increases, acknowledged by steeper curve decays of the 432 monomeric peaks.

Intriguingly, when comparing not each individual absorbance spectrum for each solution as demonstrated on Fig. 8, but the initial and final absorbance of the perylene monomer peak, the 432 nm band, an interesting trend is immediately recognized. In Fig. 9, the 432 nm absorbance values at t = 0 ms (first measured absorbance value) and t = 500 ms (final acquired absorbance value) were plotted for all seven solutions of perylene with added DMPBI. It is clear that the intensity of the 432 nm peak decreases as the addition of DMPBI
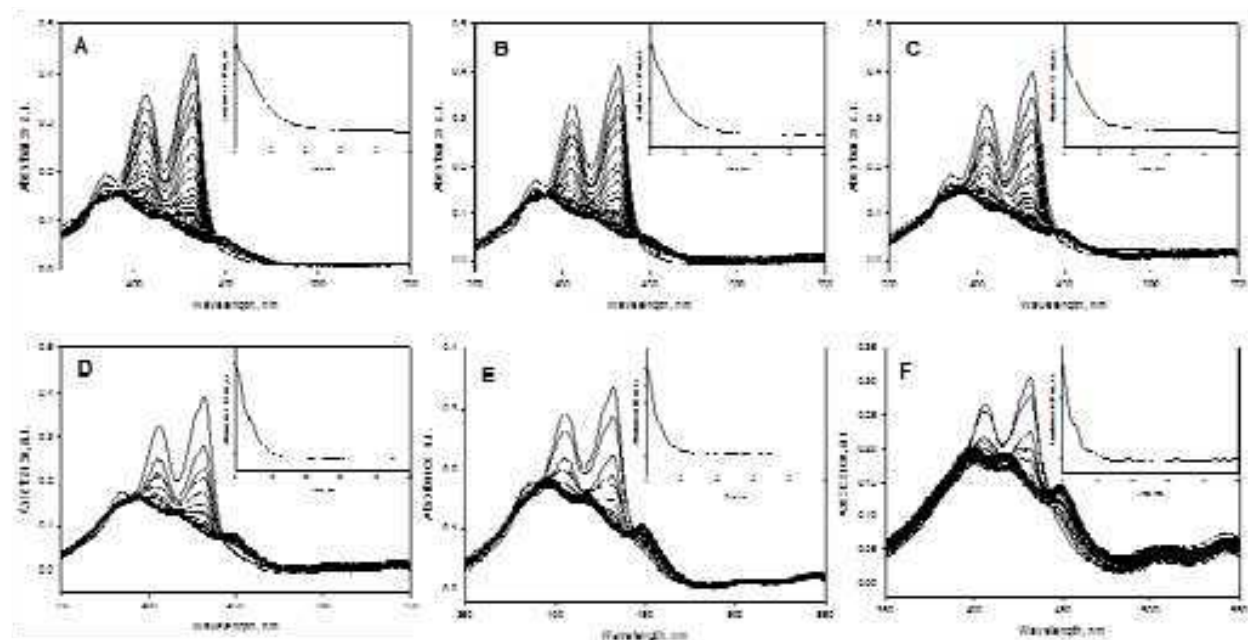
Fig. 8. Time-resolved absorption spectra of perylene in acetone after reprecipitation in water with 1%, 2%, 5%, 10%, 20%, and 30% added DMPBI (A – F, respectively). Refer to Table 1 for detailed information on the composition of solutions. Insets show absorbance decays for each added percentage of DMPBI at 432 nm (monomer consumption)
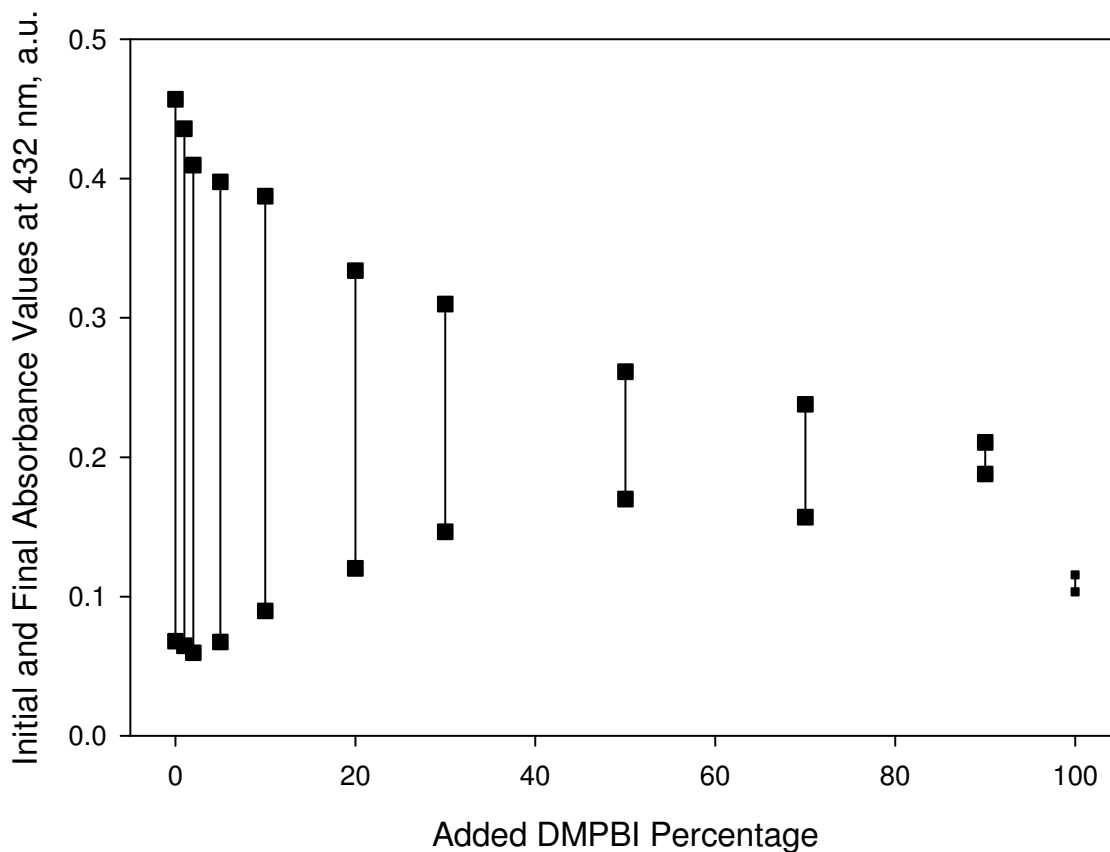

Fig. 9. Initial (t = 0 ms) and final (t = 500 ms) absorbance values at 432 nm for 0.2 mmol L^{-1} perylene in acetone mixed in water with 0%, 1%, 2%, 5%, 10%, 20%, and 30% added DMPBI

increases, more importantly, the initial value at 0 ms is progressive reaching lower absolute values as the DMPBI percentage raises from 0 to 30 percent. Because the concentration of perylene is fixed at 0.20 mmol L⁻¹ for every solution, the initial measured absorbance value is expected to be constant throughout the addition of DMPBI, since as previously discussed in Fig. 7, there is no contribution in the 432 nm spectra range due to the presence of DMPBI. The fact that the initial absorbance value is constantly decreasing with rising additive concentration is a straightforward indication that DMPBI is causing the nanocrystallization process to occur at faster rates. As stated, the dead time of the stopped flow instrument is 4 ms, which means that the initial absorbance value is actually collected 4 ms after mixing the perylene/DMPBI solution with water. For that reason, the decline in initial absorbance values are believed to be due to reactions manifesting at faster nanocrystallization rates, for perylene monomer molecules are progressively consumed at accelerated rates during the 4 ms necessary for the stopped flow initial measurement.

As previously performed on Figs. 2, 4 and 5, rates of perylene nanocrystal formation were calculated using the 432 nm peak decay. Fig. 10 shows perylene nanocrystallization rates (A), as well as the mean crystal size for perylene nanoparticles (B), as a function of added DMPBI percentage. Crystal sizes plotted on the figure were determined with the aid of the dynamic light scattering (DLS) technique. Each displayed data point, on each graph, is the average of three individual determinations.
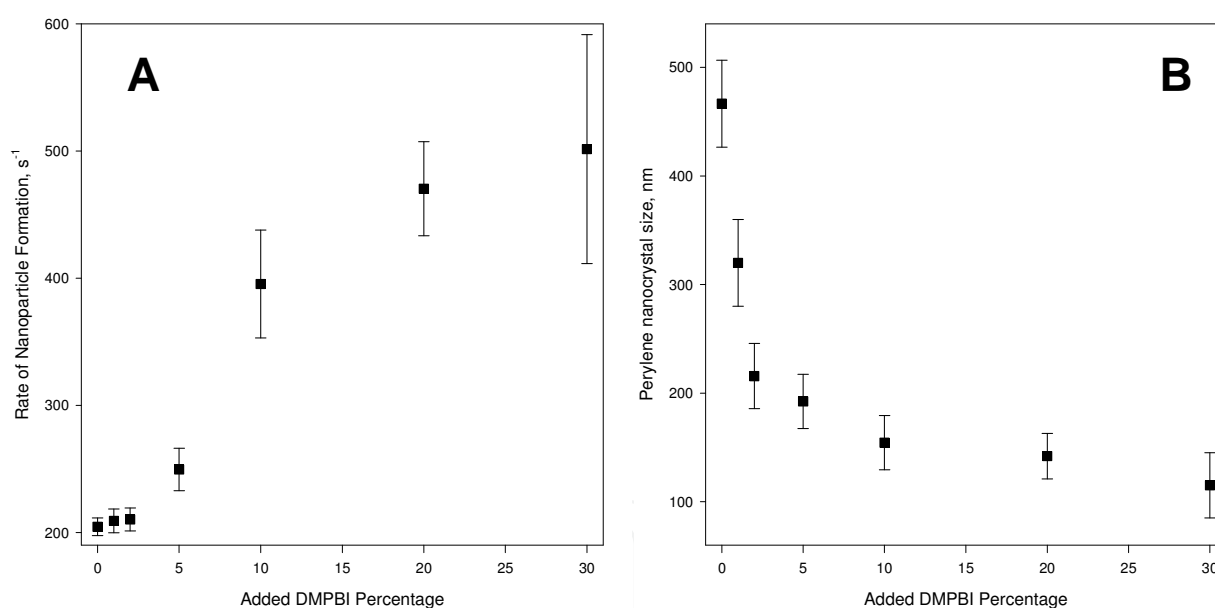

Fig. 10. (A) Rates of nanoparticle formation as a function of added DMPBI percentage for perylene 0.2 mmol L⁻¹ , and (B) Perylene nanocrystals size measured with Dynamic Light Scattering (DLS) as a function of the percentage of added DMPBI.

Undoubtedly, the formation of perylene nanoparticles by the reprecipitation method is occurring at higher rates as the concentration of DMPBI in solution increases. It should be pointed out that in Fig. 8-F (30% DMPBI addition), the 432 nm perylene monomeric peak decay has a relative low intensity, leading to larger calculated errors on its formation rate, as illustrated in Fig. 10-A. In fact, standard deviations for calculated rates of perylene nanoparticle formation were not higher than 10% when the concentration of DMPBI was kept under 20 percent. However, at 30 percent DMPBI addition, standard deviation from

three individual measurements was nearly 20%. The high errors associated with nanocrystallization rates at higher DMPBI percentages prompted experiments to be maintained at DMPBI concentrations not higher than 0.06 mmol L^{-1}, i.e., 30 percent.

The direct correlation between nanoparticle formation rates and nanoparticle sizes, makes it clear that addition of DMPBI to perylene solutions not only alters nanocrystallization rates, but is also an elegant way to manipulate sizes of perylene nanoparticles produced by the reprecipitation method, easily observed on Fig. 10-B. Comparing graphs A and B in Fig. 10, one notices that sizes of perylene nanoparticles are inversely proportional to added DMPBI concentration. When no DMPBI molecules are added to the system, perylene nanocrystals are reprecipitated with a mean size of 466.5 nm; in contrast, the addition of 30 percent DMPBI (refer to Table 1 for solution information) leads to a decrease in perylene mean particle size to about 115.1 nm.

It was suggested here that the kinetics of organic compounds'nanoparticle formation is in accordance with the classical nucleation theory. Nanoparticle formation rates of perylene, anthracene and benzo[a]pyrene (Figs. 2, 4, and 5) were calculated in solutions constituted of solvent and solute molecules only, going through what was previously named "homogeneous nucleation" (Kashchiev & van Rosmalens, 2003). In contrast, "heterogeneous nucleation"(Kashchiev & van Rosmalens, 2003) takes place in solutions having impurity molecules and/or foreign substrates that provide centers for nucleation to occur. In accordance, the introduction of DMPBI molecules, a foreign particle different from the nucleating crystalline phase, is sought to offer active centers for the heterogeneous nucleation of perylene nanoparticle to occur during the reprecipitation method.

It was formerly showed that at a given supersaturation level, homogeneous nucleation take place at lower rates than heterogeneous nucleation (Sear, 2007) since the presence of foreign substrates can act as nucleation-active centers which in turn could facilitate and thus accelerate the nucleation process. At higher nucleation rates, larger number of cluster (nuclei) are formed in solution and consequently there are less dissolved monomers available in solution for particle growth, ultimately leading to smaller sized particle.

Indeed Fig. 10 seems to indicates that DMPBI molecules indeed play the role of nucleation-active centers; indicated by the increase in nanocrystallization rates (Fig. 10-A), and consequently to the decrease in nanoparticle sizes (Fig. 10-B). Thus, it is clear that the addition of DMPBI to an organic compound solution in order to alter nanocrystallization rates is an effective method to manipulate sizes of organic nanocrystals produced by the reprecipitation method (Oliveira et al., 2010). An appropriate analogy for the role of DMPBI in organic nanoparticle formation is the extensive use of seeds in the fabrication of metallic nanoparticles, in which small metal particles are initially prepared to be later employed as "seeds" for the fabrication of larger size particle. Such process is commonly referred to "seeding growth method" (Kan et al., 2003; Yong et al., 2006), where the desired nanoparticle size can be successfully controlled by varying the ratio of seed to metal salt. In comparison, the size of prepared organic nanoparticles by the reprecipitation method seems to be controlled by simply altering the organic nanoparticle to foreign substrate (DMPBI) ratio.

To confirm nanoparticle sizes determined by DLS on Fig. 10-B, and to investigate the morphological difference in perylene nanocrystals with the addition of DMPBI, scanning electron microscopy (SEM) images were obtained for nanocrystals prepared using the stopped flow apparatus in both the presence and absence of DMPBI molecules. Fig. 11

displays SEM images of perylene nanocrystals without the addition of the organic additive, as well as with the addition of 1, 5, and 30 percent DMPBI (A-D respectively). Crystal sizes observed by SEM are similar to the average sizes obtained by DLS measurements, suggesting no association between dispersed perylene nanoparticles. Furthermore, the increasing addition of DMPBI to perylene solutions not only altered its nanocrystal size, but also modified its morphology. Spherical and cylindrical shaped nanocrystals could be seen even at 5 % DMPBI addition (Fig. 11-C), ultimately becoming the prominent shape at 30 % organic additive addition (Fig. 11-D).
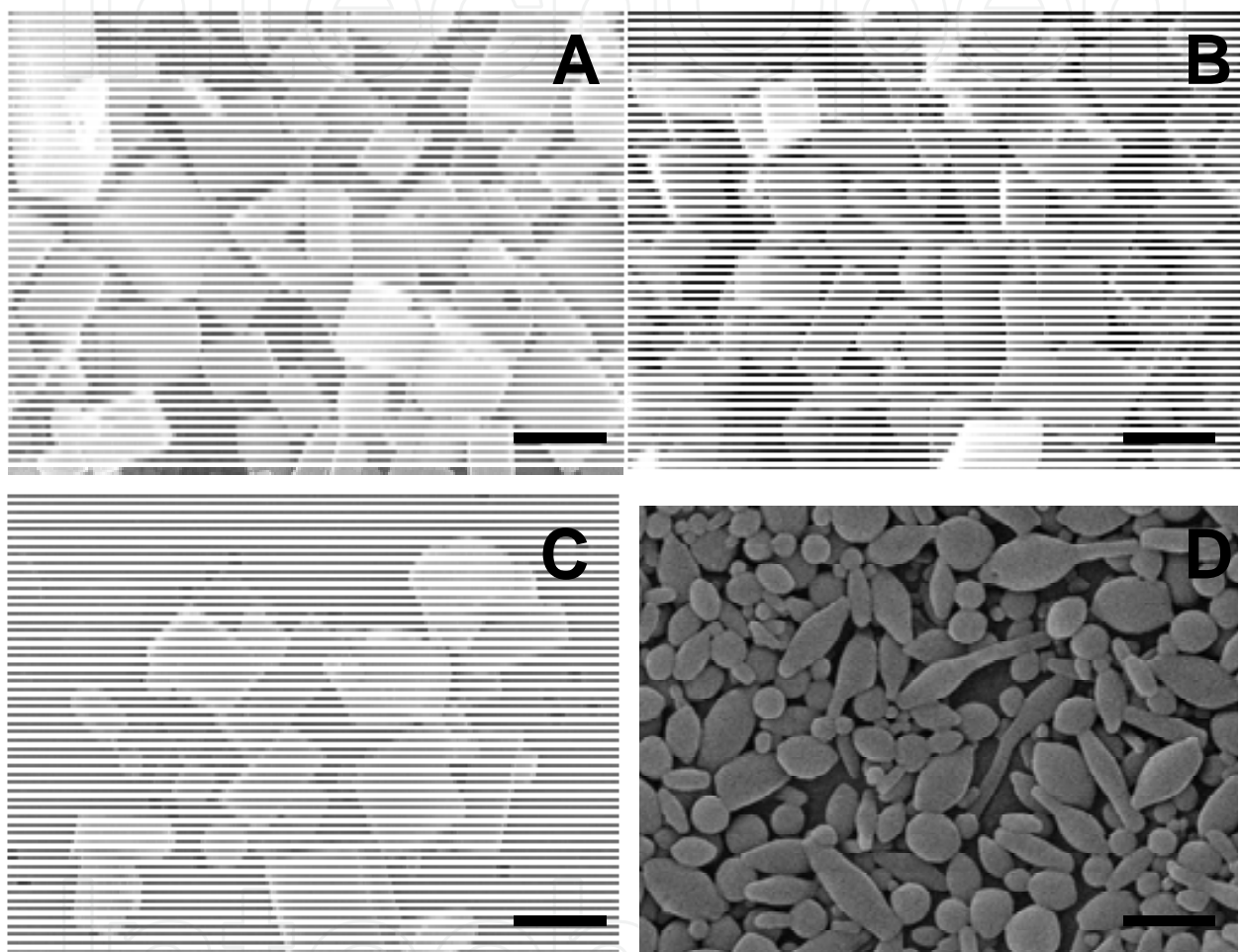
Fig. 11. SEM images of perylene nanocrystals fabricated by the reprecipitation method using the stopped-flow apparatus. (A) No addition of DMPBI, (B) 1% added DMPBI, (C) 5% added DMPBI, and (D) 30 % added DMPBI . Scale bars represent 200 nm.

3. Conclusion

Collectively, it has been demonstrated that the stopped-flow UV-Visible absorption spectroscopy technique is a promising technique for studying the *in situ* formation of organic nanocrystals by the reprecipitation method within a time frame of few milliseconds. As the vast majority of academic and industry research on the mechanism of nanosized crystal formation is focused on inorganic compounds, it was valuable to address that the stopped-flow method can be used as a tool for studying the mechanism and kinetics of organic nanoparticle formation.

The results obtained suggested that the kinetics of the organic nanomaterial formation process by the reprecipitation method qualitatively obeys the classical nucleation theory. By correlating nanocrystals growth with a well established theory, the work presented here can have a meaningful influence on future developments regarding organic nanoparticle production.

Moreover, it was clearly elucidated that it is possible to manipulate sizes of organic nanomaterials produced by the reprecipitation method by the addition of a foreign organic substrate, namely, N,N'-bis(2,6-dimethylphenyl)-3,4,9,10–perylenedicarboxyimide (DMPBI). While providing active centers for nucleation, foreign particles facilitate the nucleation process, leading to considerable acceleration in the nanocrystallization process, and ultimately to smaller sized particles.

Having specific knowledge on the mechanism of organic nanosized material production while being able to precisely and accurately control its size, material scientists can directly contribute to advancements on society by providing novel methods directed to the production of high demanded nanomaterials. For instance, high performance organic pigments and dyes can be successfully produced with controllable sizes through methods described here. Such materials are extremely industry-attractive for its use on textiles, printing inks, paint and coatings, and plastic.

4. Acknowledgment

5. References

An, B. K.; Kwon, S. K.; Jung, S. D. & Park, S. Y. (2002). Enhanced Emission and Its Switching in Fluorescent Organic Nanoparticles. *J. Am. Chem. Soc.*, Vol. 124, No. 48, (December 2002), pp. 14410-14415, ISSN 0002-7863

Auweter, H.; Haberkorn, H.; Heckmann, W.; Horn, D.; Luddecke, E.; Rieger, J. & Weiss, H. (1999) Supramolecular Structure of Precipitated Nanosize β-Carotene Particles. *Angew. Chem. Int. Ed.*, Vol. 38, No.15, (August 2009), pp. 2188-2191, ISSN 1433-7851

Baba, K.; Kasai, H.; Masuhara, A.; Okada, S.; Oikawa, H. & Nakanishi, H. (2007). Diacetylene Nanowire Crystals Prepared by Reprecipitation/Microwave-Irradiation Method. *Japanese Journal of Applied Physics*, Vol. 46, No. 11, (November 2007), pp. 7558-7561, ISSN 0021-4922

Bilgili, E.; Yepes, J. & Scarlett, B. (2006). Nano-milling of pigment agglomerates using a wet stirred media mill: Elucidation of the kinetics and breakage mechanisms. *Chemical Engineering Science*, Vol. 61, No. 1, (January 2006), pp. 149-157, ISSN 0009-2509

Blyshak, L. A.; Dodson, K.Y.; Patonay, G.; Warner, I.M. & May, W.E. (1989). Determination of cyclodextrin formation constants using dynamic coupled-column liquid chromatography. *Anal. Chem.*, Vol. 61, No. 9, (May 1989), pp. 955-960, ISSN 0003-2700

Burda, C.; Chen, X.; Narayanan, R. & El-Sayed, M.A. (2005). Chemistry and Properties of Nanocrystals of Different Shapes. *Chemical Reviews*, Vol. 105, No. 4, (March 2005), pp. 1025-1102, ISSN 0009-2665

Chaikin, P. M. & Lubensky, T.C. (1995). *Principles of Condensed Matter Physics* (1st Ed.), Cambridge University Press, ISBN 0 521 43224 3, Cambridge, UK

Chen, W. & Zhang, J. (2006). Using Nanoparticles to Enable Simultaneous Radiation and Photodynamic Therapies for Cancer Treatment. *Journal of Nanoscience and Nanotechnology*, Vol. 6, No. 4, (April 2006), pp. 1159-1166, ISSN 1550-7033

Chung, H.R.; Kwon, E.; Oikawa, H.; Kasai, H. & Nakanishi, H. (2006). Effect of solvent on organic nanocrystal growth using the reprecipitation method. *Journal of Crystal Growth*, Vol. 294, No. 2, (September 2006), pp. 459-463, ISSN 0022-0248

Debenedetti, P. G. (1996). *Metastable Liquids* (1st Ed.), Princeton University Press, ISBN 0691085951, Princeton, NJ, USA

Eisenbrand, J. & Baumann, K. (1970). Über die bestimmung der wasserlöslichkeit von coronen, fluoranthen, perylen, picen, tetracen und triphenylen und über die bildung wasserlöslicher komplexe dieser kohlenwasserstoffe mit coffein. *European Food Research and Technology*, Vol. 144, No. 5, (April 1970), pp. 312-317, ISSN 1438-2377

Frendler, J.H. (1987). Atomic and molecular clusters in membrane mimetic chemistry. *Chemical Reviews*, Vol. 87, No. 5, (October 1987), pp. 877-899, ISSN 0009-2665

Fu, H. B. & Yao, J.N. (2001). Size Effects on the Optical Properties of Organic Nanoparticles. *J Am. Chem. Soc.*, Vol. 123, No. 7, (February 2001), pp. 1434-1439, ISSN 0009-2665

Hayashi, K.; Morii, H.; Iwasaki, K.; Horie, S.; Horiishi, N. & Ichimura, K. J. (2007). Uniformed nano-downsizing of organic pigments through core–shell structuring. *Journal of Materials Chemistry*, Vol. 17, No. 6, (February 2007), pp. 527-530, ISSN 0959-9428

Horn, D. & Rieger, J. (2001). Organic Nanoparticles in the Aqueous Phase-Theory, Experiment, and Use. *Angew. Chem. Int. Ed.*, Vol. 40, No. 23, (December 2001), pp. 4330-4361, ISSN 1433-7851

Ibanez,A.; Maximov, S.; Guiu, A.; Chaillout, C. & Baldeck, P.L. (1998). Controlled Nanocrystallization of Organic Molecules in Sol-Gel Glasses. *Advanced Materials*, Vol. 10, No. 18, (December 1998), pp. 1540-1543, ISSN 0935-9648

Kan, S. H; Mokari, T.; Rothenberg, E. & Banin, U. (2003). Synthesis and size-dependent properties of zinc-blende semiconductor quantum rods. *Nature Materials*, Vol. 2, No. 3, (March 2003), pp. 155-158, ISSN 1476-1122

Kang, L.; Wang, Z.; Cao, Z.; Ma, Y.; Fu, H. & Yao, J. (2007). Colloid Chemical Reaction Route to the Preparation of Nearly Monodispersed Perylene Nanoparticles: Size-Tunable Synthesis and Three-Dimensional Self-Organization. *J Am. Chem. Soc.*, Vol. 129, No. 23, (June 2007), pp. 7305-7312, ISSN 0009-2665

Kasai, H.; Nalwa, H.S.; Oikawa, H.; Okada, S.; Matsuda, H.; Minami, N.; Kakuta, A.; Ono, K.; Mukoh, A. & Nakanishi, H. (1992). A Novel Preparation Method of Organic Microcrystals. *Japanese Journal of Applied Physics*, Vol. 31, No. 8, (August 1992), pp. L1132-L1134, ISSN 0021-4922

Kasai, H.; Kamatani, H.; Okada, S.; Oikawa, H.; Matsuda, H. & Nakanishi, H. (1996). Size-Dependent Colors and Luminescences of Organic Microcrystals. *Japanese Journal of Applied Physics*, Vol. 35, No. 2, (February 1996), pp. L221-L223, ISSN 0021-4922

Kasai, H.; Oikawa, H.; Okada, S. & Nakanishi, H. (1998). Crystal Growth of Perylene Microcrystals in the Reprecipitation Method. *Bulletin of the Chemical Society of Japan*, Vol. 71, No. 11, (June 1998) 2597-2601, ISSN 0009-2673

Kashchiev, D. & van Rosmalens, G. M. Review: Nucleation in solutions revisited. *Crystal Research and Technology*, Vol. 38, No. 7-8, (July 2003), pp. 555-574, ISSN 0323-1300

Katagi, H.; Kasai, H.; Okada, S.; Oikawa, H.; Komatsu, K.; Matsuda, H.; Liu, Z. & Nakanishi, H. (1996). Size Control of Polydiacetylene Microcrystals. *Japanese Journal of Applied Physics*, Vol. 35, No. 10B, (October 1996), pp. L1364-L1366, ISSN 0021-4922

Laaksonen, A.; Talenquer, V. & Oxtoby, D. W. (1995). Nucleation: Measurements, Theory, and Atmospheric Applications. *Annual Review of Physical Chemistry*, Vol. 46, (October 1995), pp. 489-524, ISSN 0066-426

Magdassi, S. & Moshe, M. B. (2003). Patterning of Organic Nanoparticles by Ink-jet Printing of Microemulsions. *Langmuir*, Vol. 19, No. 3, (February 2003), pp. 939-942, ISSN 0743-7033

Masuhara, H.; Nakanishi, H. & Sasaki, K. (2003). *Single Organic Nanoparticles* (1st Ed.), Springer, ISBN 3-540-00187-5, New York, USA

McWilliams, A. (July 2010). Nanotechnology: A Realistic Market Assessment. *BBC Research*, 01.07.2010, Available from http://www.bccresearch.com/report/NAN031D.html

Miyashita, Y.; Baba, K.; Kasai, H.; Nakanishi, H. & Miyashita, T. (2008). A New Production Process of Organic Pigment Nanocrystals. *Molecular Crystals & Liquid Crystals*, Vol. 492, (October 2008), pp. 268-274, ISSN 1542-1406

Mori, J.; Miyashita, Y.; Oliveira, D.; Kasai, H.; Oikawa, H. & Nakanishi, H. (2009). Stopped-flow analysis on the mechanism of perylene nanoparticle formation by the reprecipitation method. *Journal of Crystal Growth*, Vol. 311, No. 3, (February 2009), pp. 553-555, ISSN 0022-0248

Nyssen, G. A.; Miller, E. T.; Glass, T. F. & Quinn II, C. R. (1987). Solubilities of hydrophobic compounds in aqueous-organic solvent mixtures. *Environmental Monitoring and Assessmet*, Vol. 9, No.1 , (July 1987), pp. 1-11, ISSN 0167-6369

Oliveira, D.; Baba, K.; Mori, J.; Miyashita, Y.; Kasai, H.; Oikawa, H. & Nakanishi, H. (2009). Nanocrystallization Mechanism of Organic Compounds in the Reprecipitation Method by Stopped-Flow Analysis. *Japanese Journal of Applied Physics*, Vol. 48, No. 10, (October 2009), pp. 105003-1-105003-5, ISSN 0021-4922

Oliveira, D.; Baba, K.; Mori, J.; Miyashita, Y.; Kasai, H.; Oikawa, H. & Nakanishi, H. (2010). Using an organic additive to manipulate sizes of perylene nanoparticles. *Journal of Crystal Growth*, Vol. 312, No. 3, (January 2010), pp. 431-436, ISSN 0022-0248

Peters, D. (1996). Ultrasound in materials chemistry. *Journal of Materials Chemistry*, Vol. 6, No. 10, (October 1996), pp. 1605-1618, ISSN 0959-9428

Sear, R. P. (2007). Nucleation: theory and applications to protein solutions and colloidal suspensions. *Journal of Physics: Condensed Matter*, Vol. 19, No. 3, (January 2007), pp. 033101-033129, ISSN 0953-8984

Spatz, J. P.; Herzog, T.; Mossmer, S.; Ziemann, P. & Moller, M. (1999). Micellar Inorganic–Polymer Hybrid Systems - A Tool for Nanolithography. *Advanced Materials*, Vol. 11, No. 2, (March 1999), pp. 149-153, ISSN 0935-9648

Sugimoto, T. (2000). *Fine Particles: Synthesis, Characterization, and Mechanisms of Growth* (1st Ed.), Mercel Dekker, ISBN 978-0824700010, New York, USA

Tiemann M.; Weiss, O.; Hartikainen, J.; Marlow, F. & Linden, M. (2005). Early Stages of ZnS Nanoparticle Growth Studied by In-Situ Stopped-Flow UV Absorption Spectroscopy. *ChemPhysChem*, Vol. 6, No. 10, (February 2005), pp. 2113-2119, ISSN 1439-4235

Tiemann, M.; Marlow, F.; Brieler, F. & Linden, M. (2006). Early Stages of ZnS Growth Studied by Stopped-Flow UV Absorption Spectroscopy: Effects of Educt Concentrations on the Nanoparticle Formation. *J Phys. Chem. B*, Vol. 110, No. 46, (November 2006), pp. 23142-23147, ISSN 1089-5647

Tiemann, M.; Marlow, F.; Hartikainen, J.; Weiss, O. & Linden, M. (2008). Ripening Effects in ZnS Nanoparticle Growth. *J Phys. Chem. C*, Vol. 112, No. 5, (February 2008), pp. 1463-1467 , ISSN 1932-7447

Tonomura, B. I.; Nakatani, H.; Ohnishi, M.; Yamaguchi-Ito, J. & Hiromi, K. (1978). Test reactions for a stopped-flow apparatus : Reduction of 2,6-dichlorophenolindophenol and potassium ferricyanide by L-ascorbic acid, *Analytical Biochemistry*, Vol. 84, No. 2, (February 1978), pp. 370-383, ISSN 0003-2697

Van Keuren, E.; Georgieva, E. & Adrian, J. (2001). Kinetics of the Formation of Organic Molecular Nanocrystals. *Nano Letters*, Vol. 1, No. 3, (March 2001), pp. 141-144, ISSN 1530-6984

Van Keuren, E.; Bone, A. & Ma, C. (2008). Phthalocyanine Nanoparticle Formation in Supersaturated Solutions, Langmuir, Vol. 24, No. 12, (June 2008), pp. 6079-6084, ISSN 0743-7463

Vogel, A. I.; Tatchell, A. R.; Furnis, B. S.; Hannaford, A. J. & Smith, P. W. G. (1996). *Vogel's Textbook of Practical Organic Chemistry* (5th Ed.), Prentice Hall, ISBN 0582462363, London, UK

Wang, F.; Han, M.Y.; Mya, K. Y.; Wang, Y. & Lai, Y.H. (2005). Aggregation-Driven Growth of Size-Tunable Organic Nanoparticles Using Electronically Altered Conjugated Polymers. *J Am. Chem. Soc.*, Vol. 127, No. 29, (July 2005), pp. 10350-10355, ISSN 0002-7863

Yong, K.; Sahoo, Y.; Swihart, M. T. & Prasad, P. N. (2006). Growth of CdSe Quantum Rods and Multipods Seeded by Noble-Metal Nanoparticles. *Adv. Mater.*, Vol. 18, No. 15, (August 2006), pp. 1978-1982, ISSN 0935-9648
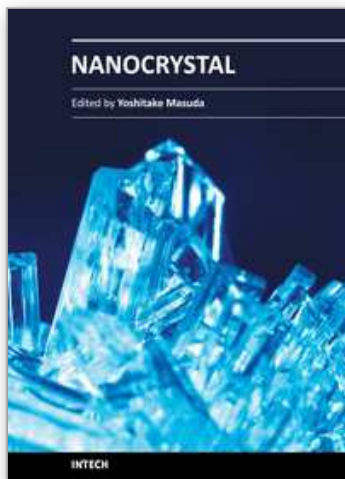
Nanocrystal

Edited by Dr. Yoshitake Masuda

We focused on cutting-edge science and technology of Nanocrystals in this book. "Nanocrystal" is expected to lead to the creation of new materials with revolutionary properties and functions. It will open up fresh possibilities for the solution to the environmental problems and energy problems. We wish that this book contributes to bequeath a beautiful environment and valuable resources to subsequent generations.

How to reference

In order to correctly reference this scholarly work, feel free to copy and paste the following:

INTECH
open science | open minds